

Simulation of Temperature Gradients and Stresses in Natural Stone Plates under Solar Radiation

H. Sadouki and F. H. Wittmann

Laboratory for Building Materials, Swiss Federal Institute of Technology,
Zürich, Switzerland

Abstract

The interaction between micro-organisms and natural stone surfaces has been studied in great detail in the past. The destructive mechanisms of micro-organisms can be roughly subdivided into (a) chemical attack and (b) physical attack. Micro-organisms may physically destroy the structure of stones by creating an inter-granular swelling pressure. Recently, it has been shown experimentally that black spots formed by yeast-like fungi lead to a local temperature increase by selective absorption of solar radiation. The maximum temperature observed for clean marble surfaces remained below the maximum temperature observed on inoculated surfaces. As a consequence, thermal dilatation of inoculated marble was shown to be more important. Destruction of the heated stone occurs predominantly if there exists a thermal gradient. In this paper, temperature distribution in clean and stained marble plates have been simulated numerically. Thermal eigenstresses have been determined. It is shown that tensile stresses of up to 5 N/mm^2 can be expected. This may cause damage in weak zones of the surface. A sudden driving rain leads to much higher stresses. Cyclic thermal loading may eventually destroy the surface by fatigue.

Key words: Natural stone, marble, thermal gradients, damage mechanism

Numerische Simulation von Temperaturgradienten und thermisch induzierten Eigenspannungen in Natursteinplatten infolge von Sonneneinstrahlung

Zusammenfassung

Seit einiger Zeit wird die Wechselwirkung zwischen Mikroorganismen und Natursteinoberflächen bis ins Einzelne gehend untersucht. Die zerstörenden Mechanis-

men der Mikroorganismen können grob in zwei Gruppen unterteilt werden: (a) chemischer Abbau und (b) physikalische Zerstörung. Mikroorganismen können oberflächennahe Zonen der Natursteine durch Quelldruck in Rissen zerstören. Kürzlich wurde experimentell nachgewiesen, dass sich Marmoroberflächen mit einer dunkel gefärbten Besiedlung durch Mikroorganismen unter Sonneneinstrahlung signifikant stärker erwärmen als Oberflächen ohne Pilzbewuchs. Als Folge davon dehnen sich die Platten mit Bewuchs thermisch stärker aus. Schädigend wirken in einer Platte in erster Linie Temperaturgradienten. In diesem Beitrag werden Temperaturverteilungen in sauberen und dunkel gefleckten Marmorplatten numerisch berechnet. Im nächsten Schritt werden die dadurch hervorgerufenen thermischen Eigenspannungen bestimmt. Es wird gezeigt, dass dabei Zugspannungen bis zu 5 N/mm^2 nachweisbar sind. Dadurch kann der Werkstoff in schwachen Zonen bereits geschädigt werden. Wesentlich höhere Zugspannungen treten auf, wenn die vorgewärmte Marmorplatte von Schlagregen getroffen wird. Eine zyklische thermische Belastung kann allmählich zur Zerstörung der oberflächennahen Zonen durch Werkstoffermüdung führen.

Stichwörter: Naturstein, Marmor, thermische Gradienten, Schadensmechanismus



Dr. Hamid Sadouki, Diploma in Physics in 1977 and PhD in Materials Science in 1987 from the Swiss Federal Institute of Technology in Lausanne. Since 1988 research scientist at the Institute of Building Materials of the Swiss Federal Institute of Technology in Zürich. Research of main interest: numerical modeling of moisture and heat transfer and fracture mechanics in porous composite materials.



Prof. Dr. F.H. Wittmann, Member of WTA, first studied physics at the universities of Karlsruhe and Munich, Germany, and in 1969 habilitated in civil engineering at University of Technology in Munich. Since 1976, he has been holding the position of professor for building materials, first at Delft, Netherlands, subsequently at EPF Lausanne, Switzerland, and presently at Swiss Federal Institute of Technology (ETH) Zürich, Switzerland. His main interest and experience are in the fields of cement-based materials and application of fracture mechanics.

1 Introduction

Micro-organisms may cause damage of mineral building materials in different ways. By producing acids, they can chemically attack the surface. By growing into cracks or pores of a material, they may cause swelling pressure high enough to induce mechanical damage.

Recently, Dornieden et al. [1] showed that optical properties of a marble surface are changed considerably by fungal growth. Absorption of solar light is increased enormously by black spots. As a consequence, the darkened surface heats up more severely under solar radiation. Therefore, the question arises if next to the damage mechanisms mentioned above, thermally induced stresses may cause noticeable damage to building materials. Uniform heating of a specimen within the range does not necessarily cause damage, but temperature gradients may be at the origin of tensile stresses.

In this contribution, temperature distributions in marble slabs are calculated numerically. The numerical model allows us to study the influence of material properties, geometry, and boundary conditions in a systematic way. It is possible to outline critical conditions for surface damage by this parameter study.

The model is applied to simulate thermal stresses in marble in the first place, but it can also be used to predict the behaviour of other mineral materials, such as light sand stone or white concrete, under solar radiation.

2 Heat evolution in a plate exposed to solar radiation

2.1 Solar radiation

Solar radiation on opaque and absorbing surfaces of a building element may have an important influence on its thermal behaviour. When the receiving surfaces are opaque, radiation is partially reflected and partially absorbed. This causes a rise in surface temperature. The effect of solar radiation on a body is complex, since the rate at which energy is delivered is highly variable with geographical latitude, time of the year, time during the day, wheather, surroundings, orientation and absorption of the receiving surfaces [2]. The intensity of the absorbed radiant energy can be expressed by the following equation:

$$q_s = I_s \cdot \cos\varphi \cdot \alpha \quad (1)$$

where:

I_s : solar energy at the earth's surface

φ : angle of incidence of the sun rays on the exposed surface
 α : absorption coefficient of the surface

Fig. 1 shows a measured curve describing the evolution of the intensity I_s of the solar radiation received by a dark horizontal surface as function of solar time. This curve represents mean values as recorded in Zürich in June between 1963 and 1972 [3].

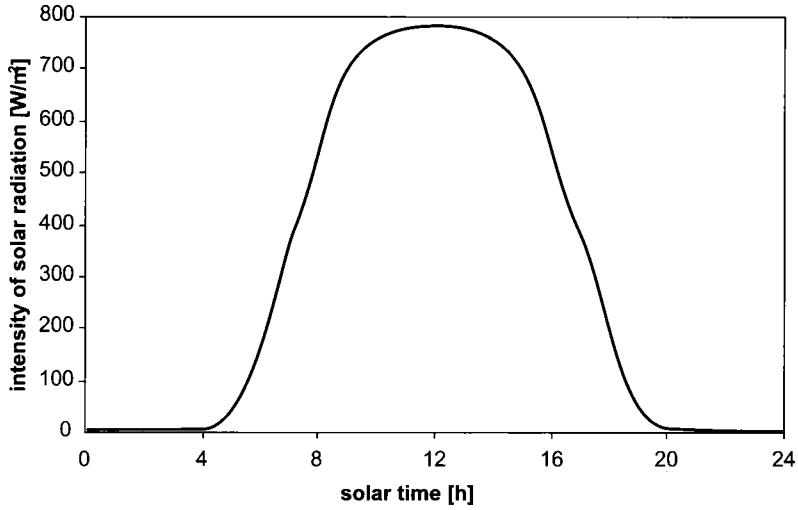


Fig.1: Intensity of solar radiation as function of time

2.2 Heat exchange with a solid body

The heat exchange between a solid body and its surrounding atmosphere is generally described by means of convective and radiative boundary conditions.

The convective heat flux \vec{q}_c at the boundary Γ of the solid Ω can be approximately described by the following equation:

$$\vec{q}_c = h_c \cdot (T_\Gamma - T_a) \cdot \vec{n} \quad (2)$$

where,

h_c : convective surface film coefficient, depending mainly on the air flow

T_Γ : temperature at the boundary Γ

T_a : temperature of the surrounding atmosphere

\vec{n} : unit vector normal to the boundary Γ

The radiative heat flux \vec{q}_r at the boundary Γ is given by the Stefan-Boltzmann law:

$$\vec{q}_r = \sigma \cdot \varepsilon \cdot \left[(T_\Gamma^K)^4 - (T_a^K)^4 \right] \vec{n} \quad (3)$$

where,

T_Γ^K and T_a^K are temperatures at the surface Γ and of the surrounding air, respectively, expressed in degree Kelvin

ε : emissivity of the surface

σ : Stefan-Boltzmann's constant

In the heat-flow theory [4] Eq. 3 can be expressed in terms of coefficient h_r as follows:

$$\vec{q}_r = h_r \cdot (T_\Gamma - T_a) \cdot \vec{n} \quad (4)$$

where,

T_Γ and T_a have the same meaning as in Eq. 2

h_r : radiative film coefficient

so that the combined convective and radiative heat exchange at the surface is given by

$$\vec{q}_{cr} = h \cdot (T_\Gamma - T_a) \cdot \vec{n} \quad (5)$$

and

$$h = h_c + h_r \quad (6)$$

2.3 Temperature profiles

The transient heat transfer process in an isotropic medium is governed by the well known Fourier's law which is expressed by the following partial differential equation:

$$c_v \frac{\partial T(\vec{X}, t)}{\partial t} = \text{div}(\lambda \cdot \text{grad} T(\vec{X}, t)) \quad (7)$$

in volume Ω

where:

$T(\vec{X}, t)$: temperature at time t at a given position \vec{X} in the volume Ω

c_v : volumetric heat capacity

λ : coefficient of thermal conductivity

Temperature profiles in the solid body at different times can be determined by solving Eq.7 combined with the aforementioned boundary conditions and assuming adequate initial conditions.

3 Numerical modelling

The non-linear finite element programm MARC [5] has been used to simulate the transient heat transfer in 3D. The thermal analysis is performed for prismatic marble specimens with varying dimensions. Fig. 2a and 2b show the idealization of the geometry of two different specimens by means of eighth-noded cube finite elements. In these idealizations, one fourth of the plates is considered. This means that faces AA'BB' and BB'CC' are plains of symmetry. Heat exchange between the specimen and its surrounding atmosphere takes place through the upper surface A'B'C'D'. It has also been assumed that only this surface is exposed to sun radiation. No heat flux is allowed through the remaining surfaces. Black marks, characterized by perfect thermal absorption (no reflection), are placed on the exposed surface in order to simulate for instance the effect of black yeast-like fungi which may be present on building materials such as marble, sandstone or concrete subject to microbiological attack. The remaining area of the exposed surface is assumed to have an absorption coefficient of 30%.

During the transient heating process, thermal gradients will develop in the specimen, causing differential deformations. If a hypothetical fiber of the material is free to expand under an infinitesimal increase ΔT in temperature, the resulting

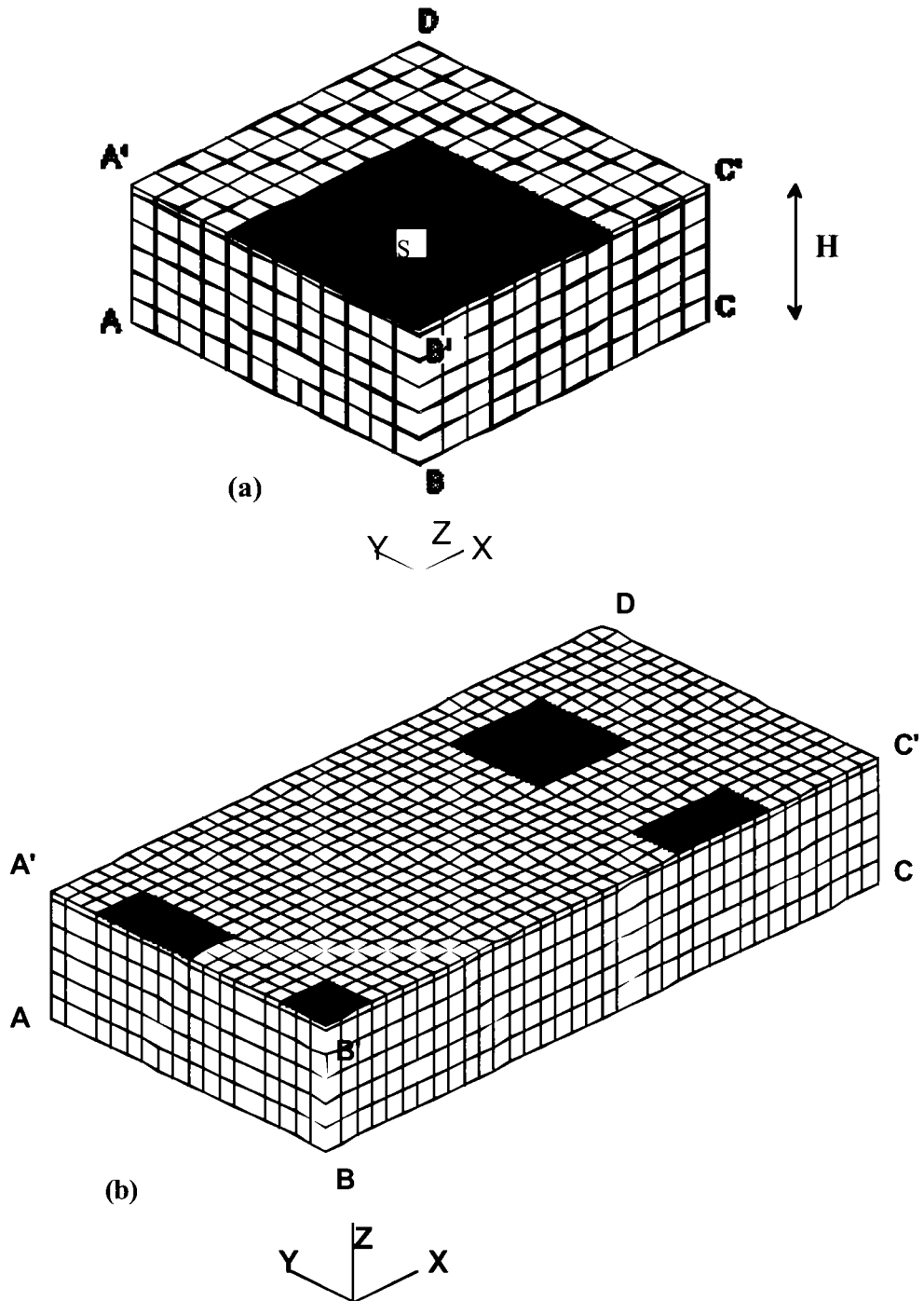


Fig. 2: Finite element idealization of the stone plates:
 (a) on black mark at center and (b) nine black marks distributed on the surface

unrestrained expansion can be computed as follows:

$$\Delta \epsilon_{th} = \alpha_{th} \cdot \Delta T \quad (8)$$

where

$\Delta \epsilon_{th}$ is the unrestrained thermal expansion and α_{th} is the coefficient of thermal expansion of the material. The internal restraint in a section under a thermal gradient will generate eigenstresses. In case the fiber is restrained to expand freely, the resulting stress σ_{th} in the linear elastic regime can be calculated by the following expression:

$$\sigma_{th} = E \cdot \alpha_{th} \cdot \Delta T \quad (9)$$

where E is the Young's modulus of the material.

The combined heat flow and stress analysis is performed with MARC [5]. The calculated time-dependent temperature distribution from the transient heat flow analysis is stored in a file for every time step Δt . For the stress analysis, the incremental thermal load ΔT is converted to a strain field via the thermal coefficient of expansion α_{th} (Eq.8). In this contribution, the material is assumed to behave in a linear-elastic manner without crack formation. This is a simplifying assumption but it does not limit the scope of this work. Formation of thermally induced cracks can be simulated if needed at later stage.

In all the following analyses, thermal variations were considered as the only origin for stress development. In principle hygral gradients can be superimposed to the thermal gradients. Time zero at which the exposure starts corresponds to 8 hours of the solar time (see Fig.1). At that time, the plate is assumed to be in a thermal equilibrium at 20 °C. Point B in Fig.2a and 2b is assumed to be fixed in all directions. That means warping of the plate may take place.

4 Material parameters

Some relevant physical parameters of marble as given by different authors are compiled in Table I [6-9].

In Table I, the letters have the following meaning:

E: Modulus of elasticity

ν : Poisson ratio

f_s : splitting tensile strength
 f_r : flexural tensile strength
 a : coefficient of linear thermal expansion
 l : thermal conductivity
 c_m : heat capacity by unit of mass

Tab. I: Physical properties of marble

E [kN/mm ²]	ν [-]	f_s [N/mm ²]	f_r [N/mm ²]	α [10 ⁻⁶ °C ⁻¹]	λ [J/mm h °C]	c_m [J/g]	Ref
49-91	0.22-0.31	4-10	-	4.2-21.9	-	-	[6]
65-105	-	7-20	-	4-8	6.7-10.5	-	[7]
30-60	-		6-15	4.7-11.2	-	0.85	[8]
20-50	-	-	8.2-31		2.7-5.1		[9]

As it can be seen, material parameters show a very wide scatter. This is generally observed for all natural stones. This large variability can be explained by the fact that all properties are directly related to the mineralogical composition and to the texture of the material. These two characteristics are strongly dependent on the genesis of the stone.

The following values have been selected and are used in the numerical simulations: $E=60\text{kN/mm}^2$, $\nu=0.25$, $a=10 \cdot 10^{-6} \text{ °C}^{-1}$, $l=8 \text{ J/mm.h. °C}$ and $C_m=0.85 \text{ J/g}$.

5 Results

5.1 Plate with one single spot

In this study, the plate with a single centered black spot as shown in Fig.2a is considered. The length of the specimen with a square shaped cross section is assumed to be 500 mm. The height is considered as a variable. The surrounding air-temperature is considered to be fixed at 30°C in all cases. The upper surface is exposed to solar radiation which is described by the curve given in Fig.1.

In Fig. 3, the simulated temperature distributions at three different exposure times ($t = 1, 7$ and 9.5 hours) are shown for a plate with a height of 100mm and a black spot at the upper exposed surface with an area of 66.67% of the total surface. It is clear, that during this transient process, the region situated at the centre of the black mark (point B' in Fig.2a) always shows the highest temperature. As it can be seen, time-dependent thermal gradients develop in all directions of the solid body. As a consequence, eigenstresses will be induced. The corresponding simulated stress contours in direction \vec{X} , σ_{xx} , are shown in Fig. 4. The tensile stress peak occurred at about 7 hours (15 hours in terms of solar time), at the node A' (see Fig. 2a). For a reason of symmetry, this peak is situated at point C' in the direction \vec{Y} (σ_{yy}). During this process, shear stresses and stresses in the direction \vec{Z} never exceeded 2 N/mm^2 .

In order to quantify the influence of the related area of the black spot on the temperature evolution in the body, the black area is now increased gradually from 0 to 100% . The height of the plate is fixed to be 100 mm . The simulated temperature histories at the node B' (Fig. 2a) are shown in Fig. 5. The highest temperature is, of course, reached when the exposed surface is fully covered by a black mark ($S=100\%$). Fig. 6 shows the induced tensile stress peaks as function of the related area of the black spot (S). In the case of the chosen geometry (height= 100mm), the highest thermally induced tensile eigenstress occurs when the related area of the black spot is roughly 60% of the total surface. For the two extreme cases ($S=0\%$ and $S=100\%$), stresses in plains normal to the \vec{Z} direction are zero, because no thermal gradients can occur in these plains.

In a further analysis, the height of the plate shown in Fig. 2a is varied from 30 to 200 mm , the related area of the black spot is fixed to be 66.67% . The simulated temperature evolutions are shown in Fig. 7 for node B' of Fig. 2a. The resulting tensile stress peak as function of the height is plotted in Fig. 8. The value of the maximal induced tensile stress is strongly dependent on the height of the plate. The thinner the plate is the higher will be the tensile stress caused by differential heating.

A further simulation has been performed in order to compare the results to experimental findings published recently by Dornieden et al. [1]. A small plate of marble with a square cross section with a length of 10 mm and a height of 3 mm is considered. Two cases are analyzed, in the first case the surface exposed to solar radiation is assumed to be totally blank (with an absorption coefficient of 30%), while in the second case, the surface is assumed to be totally covered by a black crust (coeff. of absorption 100%).

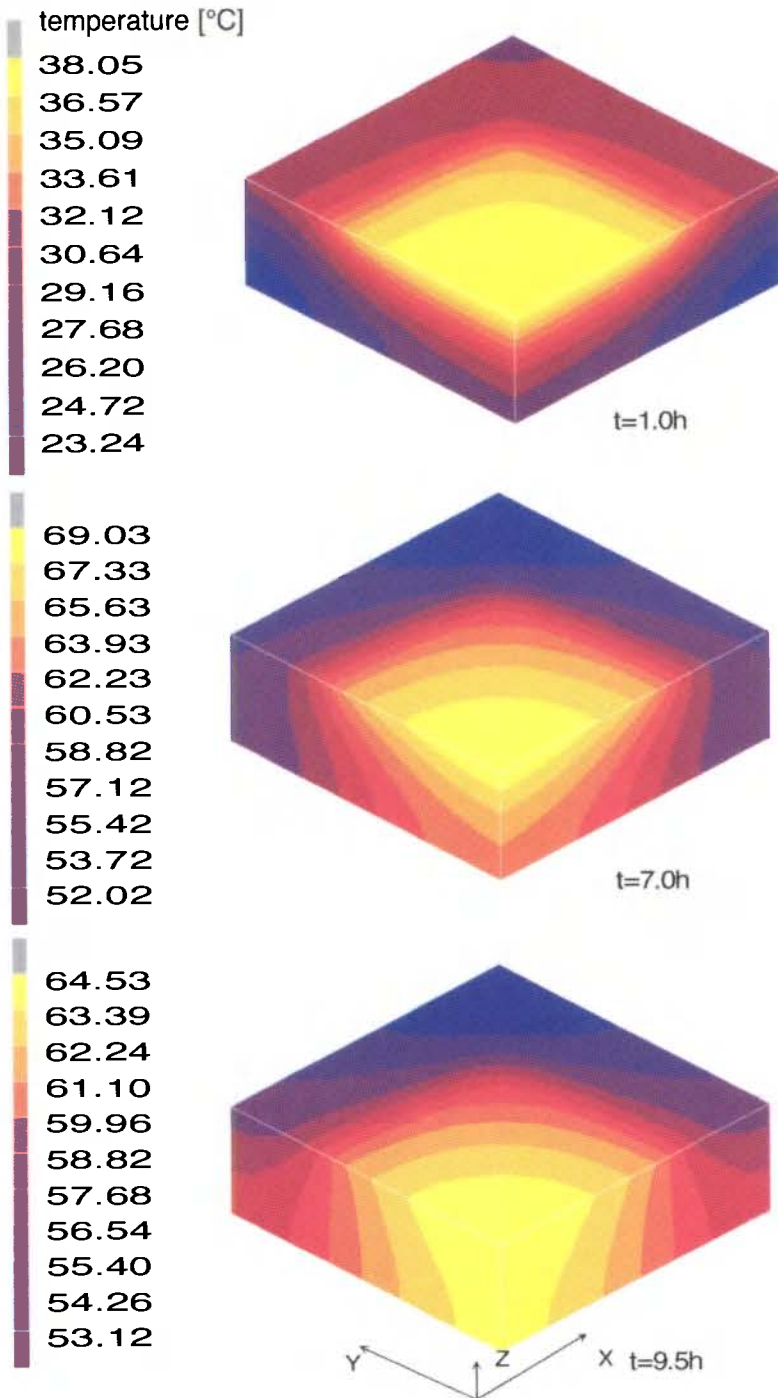


Fig. 3: Simulated temperature contours for three different times of exposure (1, 7 and 9.5 hours)

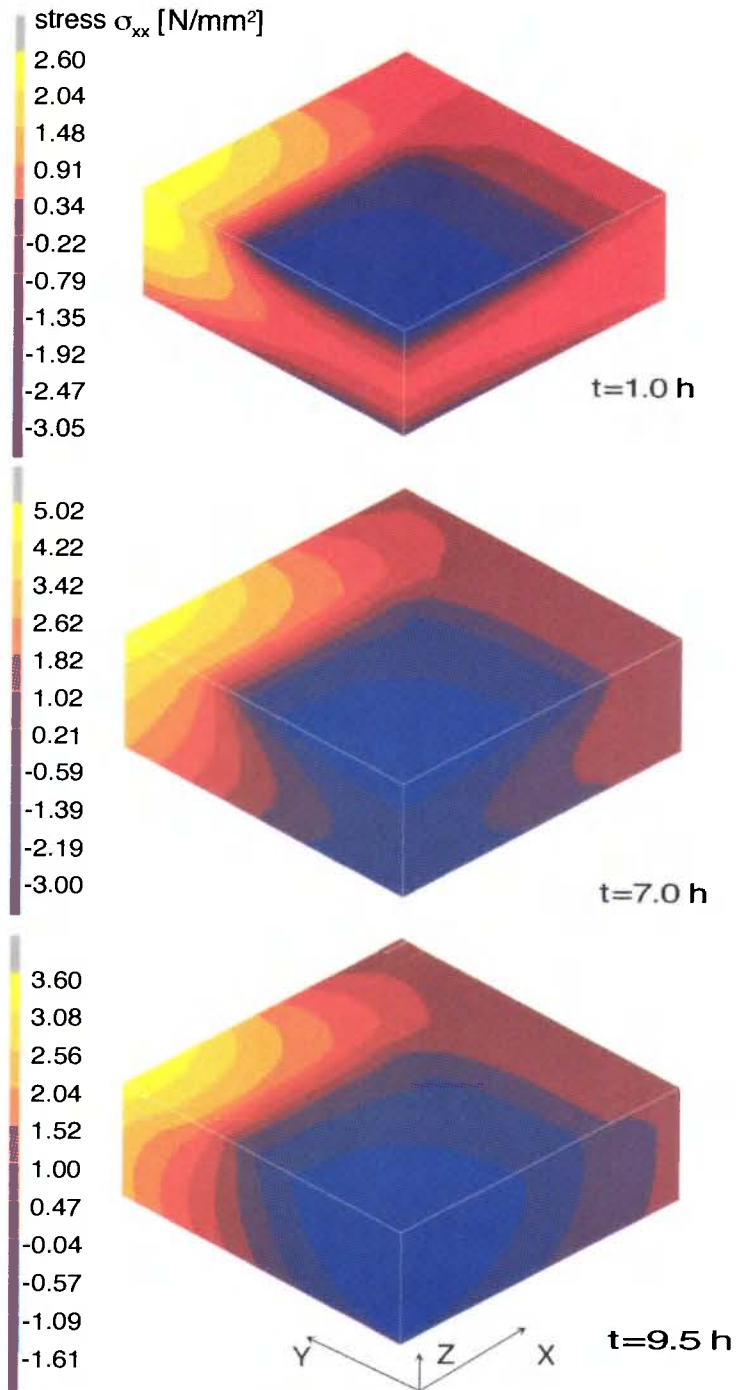


Fig. 4: Simulated stress contours in the direction X for different times of exposure (1, 7 and 9.5 hours)

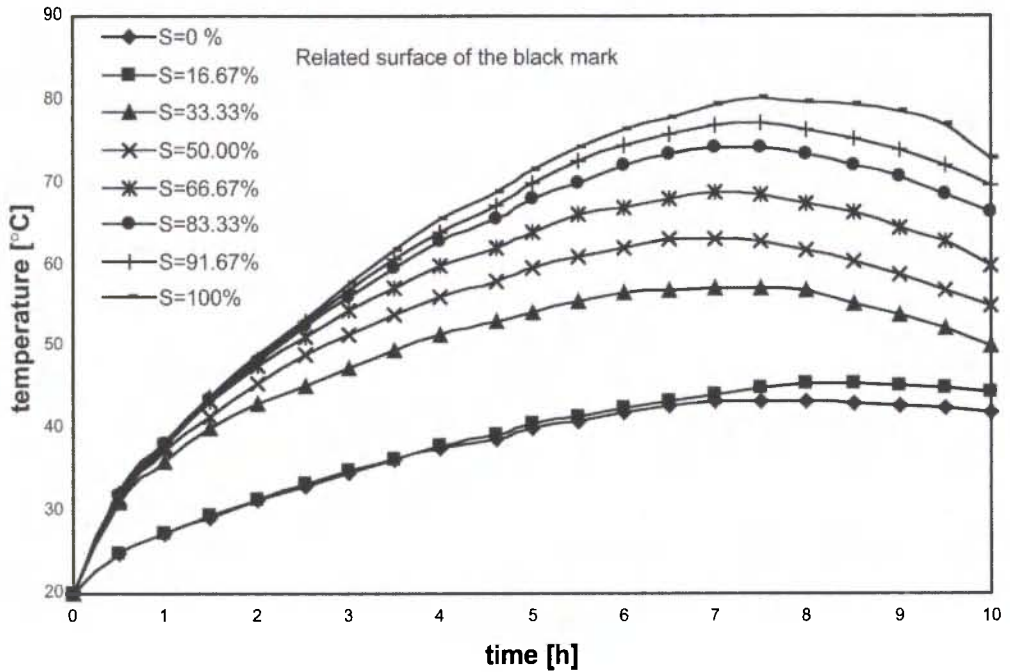


Fig. 5: Temperature evolution for node B' of Fig. 2a, for different relative area of the black mark

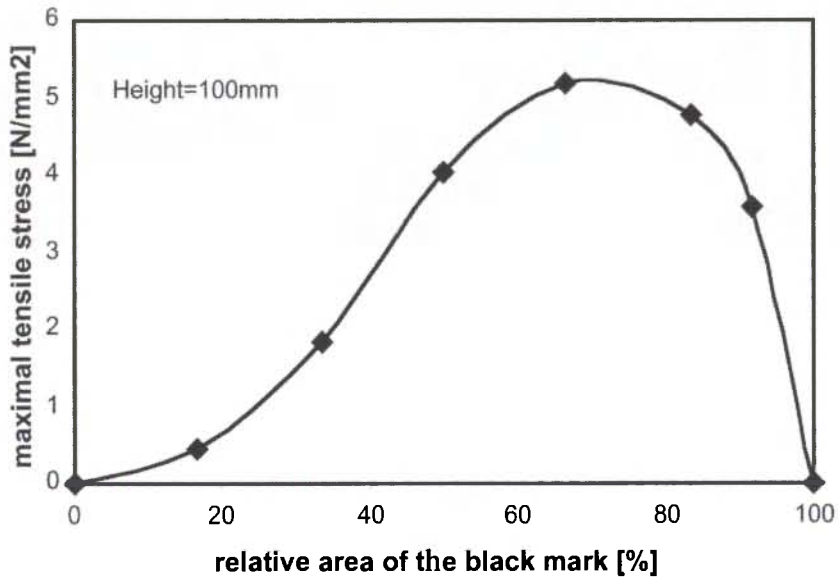


Fig. 6: Tensile stress peak as function of the relative area of the black spot

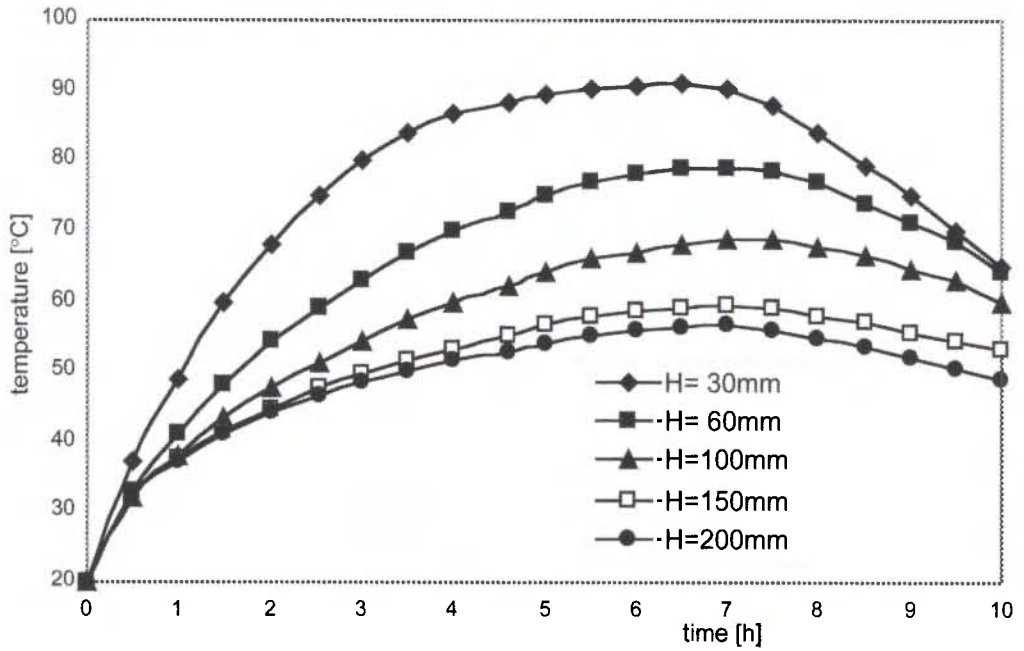


Fig. 7: Temperature evolution for node B' of Fig. 2a for different heights of the plate

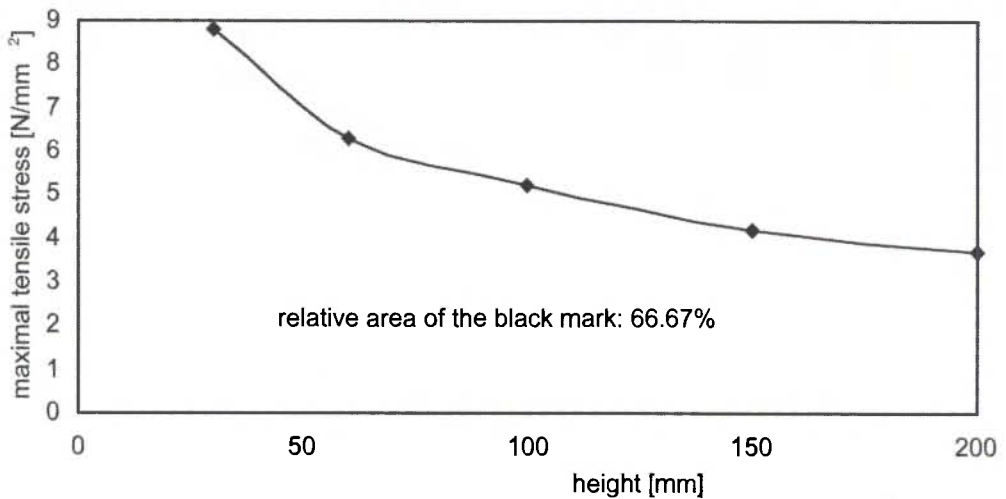


Fig. 8: Tensile stress peak as function of the height of the plate

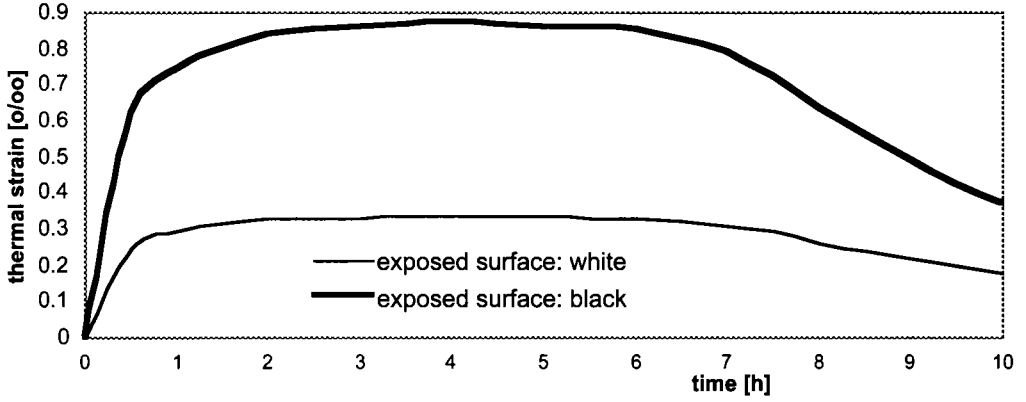


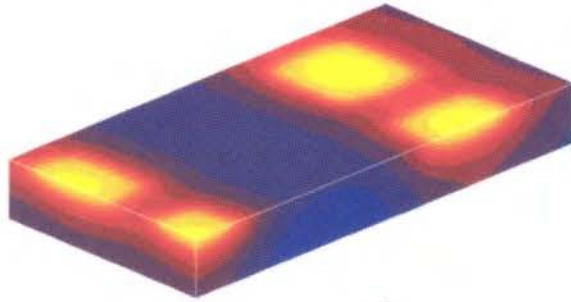
Fig. 9: Thermal strain as function of exposure time

Fig. 9 shows for both cases the evolution of the relative thermal expansion as function of the exposure time. The thermally induced strain in the first case is roughly three times lower than in the second one. This comparison of course cannot be very precise. The physical properties of the marble used in the experiments [1] are unknown. They can be quite different as compared to those chosen for the numerical simulation. Nevertheless it can be seen that the order of magnitude is correct.

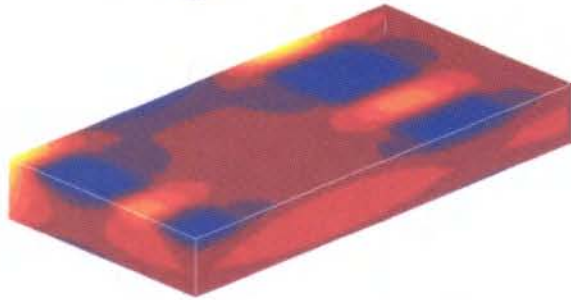
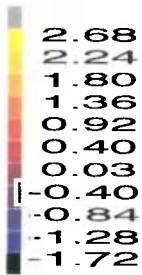
5.2 Plate with nine spots

In order to study the interaction of several black marks on one surface, a simple model as shown in Fig. 2b is considered. The length, the width and the height of the plate are fixed and assumed to be 1000, 500 and 100 mm, respectively. Because of symmetry reasons, one fourth of the plate is considered only. On the upper surface exposed to solar radiation, nine dispersed black spots with equal areas are assumed. The area of each spot is considered as a variable. Initial and boundary conditions are the same as those used in the case of one single spot. In Fig.10, the simulated temperature distribution and the induced eigenstresses in the directions \bar{X} , \bar{Y} and \bar{Z} ($\sigma_{xx}, \sigma_{yy}, \sigma_{zz}$) are shown at one exposure time of 6.8 hours. At that time the highest tensile stresses occur. Fig. 10 corresponds to the spot configuration causing the highest tensile stresses. This means that an increase or a decrease

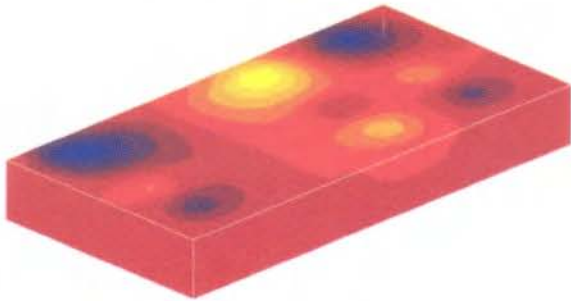
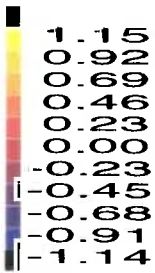
temperature [°C]



σ_{xx} [N/mm²]



σ_{yy} [N/mm²]



σ_{zz} [N/mm²]

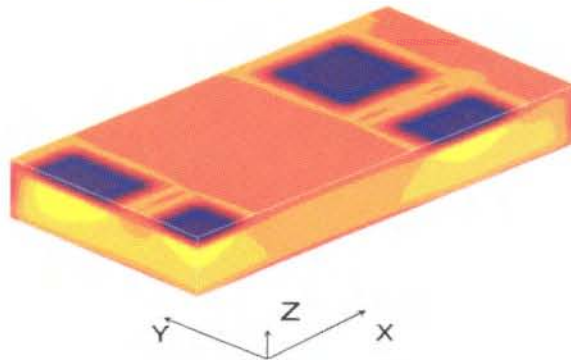
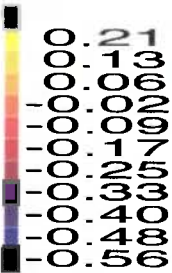


Fig. 10: Simulated contours for temperature and normal stresses for a plate with nine black spots

of the spot areas will induce lower tensile stresses. This value can be much higher, however, if the height of the plate is reduced. This has been shown already in the analysis with one single spot (see Fig.8).

5.3 Effect of driving rain

As it can be seen from the above analyses, solar radiation absorbed by black spots situated on an exposed surface of a marble plate can induce high temperatures in the solid body. The highest temperature occurs on the upper layer near the surface. If the hot surface is suddenly cooled down, by example by a driving rain, high tensile stresses will be generated.

In the following analysis this thermal shock is simulated by using the model of one single spot of Fig. 2 (height=100mm, related area of the spot=66.67%). The upper surface is assumed to be exposed to solar radiation during 7 hours. At that time a sudden driving rain starts to hit the plate. In the numerical modelling, the effect of driving rain is simulated by assuming that the exposed surface is in contact with water of 5°C. The heat exchange between water and the plate is governed by convection. In reality, the situation may be considerably more severe. The porous material can absorb cold water. In this case hygral and thermal stressses have to be taken into consideration. The simulated temperature histories are plotted in Fig. 11 for nodes A', B and B' (see Fig. 2.a). Nodal temperature evolutions of the first 6 hours of the warming up periode are omitted in Fig. 11. A sudden drop in temperature at the upper surface occurs, while the deeper layers cool

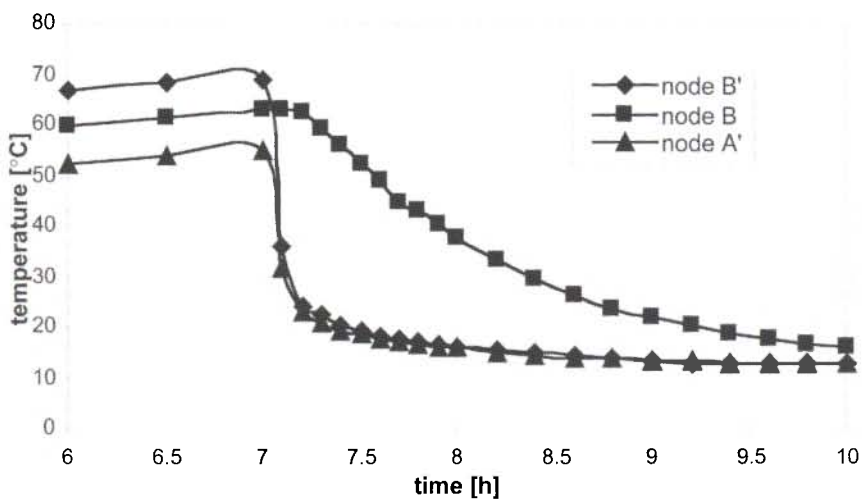


Fig.11: Nodal temperature evolution when the upper surface of the plate is subject to sudden cooling.

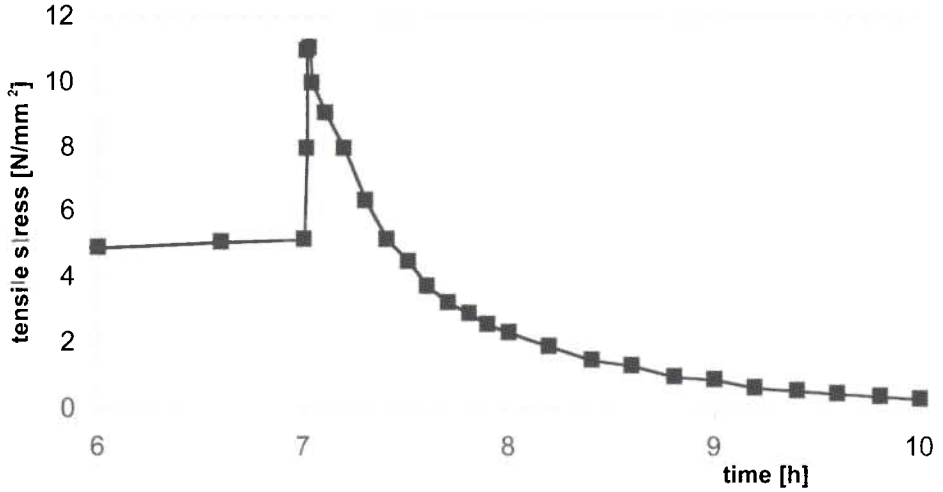


Fig.12: Tensile stress evolution at the corner A' when the upper surface of the plate is subject to sudden cooling.

down slowly. The time evolution of the tensile stress in the direction \vec{X} at the corner A' is given in Fig.12. As it can be seen a sudden jump of stress, induced by the contact with driving rain, occurs.

6 Discussion and Conclusions

The effect of black spots on the thermo-mechanical behaviour of marble plates exposed to solar radiation is simulated by means of a 3 D numerical model.

The temperature in a marble plate can be very high if the exposed surface of the solid body is covered by black spots. Depending on the geometry of the element and on the related area of the black marks, the temperature can be up to 40 °C higher as compared to case of a blank marble plate.

Thermal gradients develop between blank and black regions of the plate, leading to eigenstresses.

The performed simulations indicate that the thermal gradients can induce considerable tensile stresses. The actual values of the tensile stresses are strongly dependent on the geometry of the solid and on the physical parameters of the material. In some cases, these stresses can be high enough to provoke locally intergranular decohesion in the material.

A brutal cooling down of a marble plate, previously subjected during some hours to solar radiation, induces high tensile stresses which can exceed the tensile strength of the material and consequently this may lead to crack formation.

In case of natural stones or other building materials such as white concrete, characterised by a high coefficient of reflection and a low tensile strength, black yeast-like fungi can locally compromise the durability of a structural element.

Estimated physical properties of marble have been introduced in this numerical modelling. There is a need to perform experiments on stones with well-defined physical properties, in order to validate the model.

References

1. T. Dornieden, A. A. Gorbushina und W. E. Krumbein: *Änderungen der physikalischen Eigenschaften von Marmor durch Pilzbewuchs*, Int. Zeitschrift für Bauinstandsetzen, 3., 441-456, (1997).
2. N.B. Hutcheon and G.O.P. Handegord: *Building Science for Cold Climate*, Nta. Res. Council of Canada, (1983).
3. H. H. Hauri und Ch. Zürcher: *Moderne Bauphysik*, Verlag der Fachvereine an den Schweizerischen Hochschulen und Techniken, Zürich, 2. Auflage, (1984).
4. H. S. Carslaw and J.C. Jaeger: *Conduction of Heat in Solids*, Oxford Science Publications, 2nd Ed., 1(1993).
5. MARC Analysis Research Corporation, *User's Manuals*, Version 6.3, Palo Alto, CA, USA, (1995).
6. U. Zezza, E. Previde Massara, V. Massa and D. Venchiarutti: *Effect of Temperature on Intergranular Decohesion of Marbles*, Proceedings of the 5th Int. Congress on Deterioration and Conservation of Stone, pp. 131-140, Lausanne, Switzerland, (1985).
7. A. Peschel: *Natursteine*, Deutscher Verlag für Grundstoffindustrie, Leipzig, Deutschland, (1977).
8. D. K. Doran, *Construction Materials Reference Book*, ed. By D.K. Doran, Butterworth Heinemann, (1992).
9. F. H. Wittmann, *Physik poröser Natursteine*, Bautenschutz und Bausanierung, 2., 4-7, (1979).

